Supporting Information

Optimizing Linear Polymer Affinity Agent Properties for Surface-enhanced Raman Scattering Detection of Aflatoxin B1

Victoria M. Szlag[†‡], Rebeca S. Rodriguez[†‡], Seyoung Jung[‖], Marc R. Bourgeois[§], Samuel Bryson[†], Anatolii Purchel[†], George C. Schatz[§], Christy L. Haynes*[†], Theresa M. Reineke*[†]

*Email: chaynes@umn.edu, Phone (work): 612-626-1096, Fax: 612-626-7541

*E-mail: treineke@umn.edu. Phone (work): 612-624-8042, Fax: 612-626-7541

[†] Department of Chemistry and [‖]Department of Chemical Engineering and Materials Science, University of Minnesota, 207 Pleasant Street SE, Minneapolis, Minnesota 55455, United States
[§]Department of Chemistry and International Institute for Nanotechnology, Northwestern University, 2145 Sheridan Road, Evanston, Illinois 60208 United States

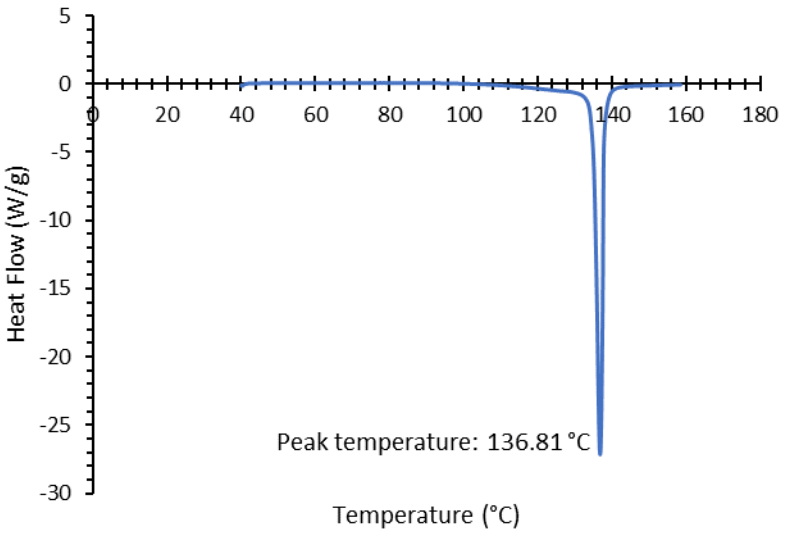

Figure S1. Differential Scanning Calorimetry (DSC) of NAGA monomer displaying T_m.

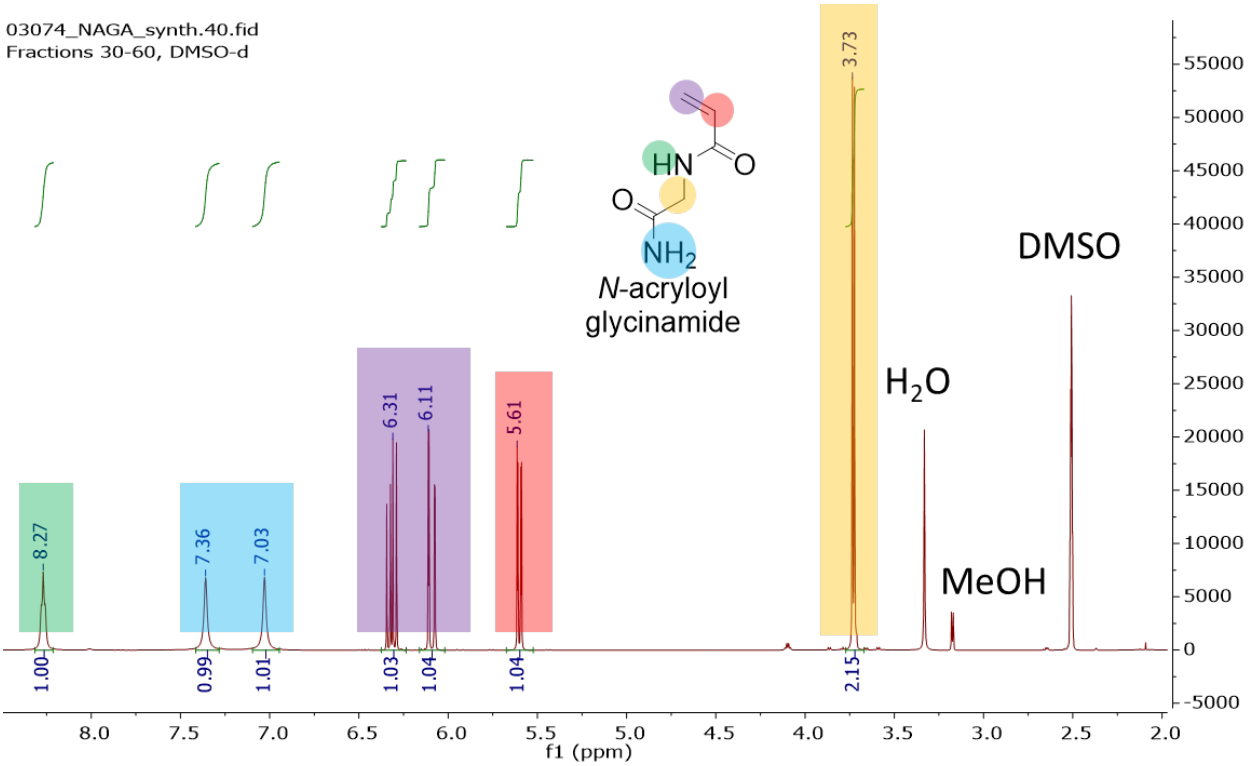

Figure S2. 1H NMR of NAGA monomer displaying NAGA synthesis reaction and NMR peak assignments.

Table S1. Polymerization reaction specifics, including molar concentrations of the monomer of N-acryloyl glycinamide (NAGA), initiator 4,4'-azobis(4-cyanovaleric acid) (V501), and chain transfer agent (CTA) 4-cyano-4-(propylsulfanylthiocarbonyl)sulfanylpentanoic acid (CPP).

Polymer	Monomer	Initiator	CTA	Additional DMSO
$pNAGA_{13}$	8.375 mL of 0.44 M NAGA in DMSO	313 µL 0.18 M V501 in DMSO	385 µL 0.43 M CPP in DMSO	0 µL
$pNAGA_{19}$	8.375 mL of 0.44 M NAGA in DMSO	209 µL 0.18 M V501 in DMSO	257 µL 0.43 M CPP in DMSO	232 µL
$pNAGA_{28}$	8.375 mL of 0.44 M NAGA in DMSO	156 µL 0.18 M V501 in DMSO	192 µL 0.43 M CPP in DMSO	350 µL
$pNAGA_{33}$	8.375 mL of 0.44 M NAGA in DMSO	124 µL 0.18 M V501 in DMSO	154 µL 0.43 M CPP in DMSO	420 µL

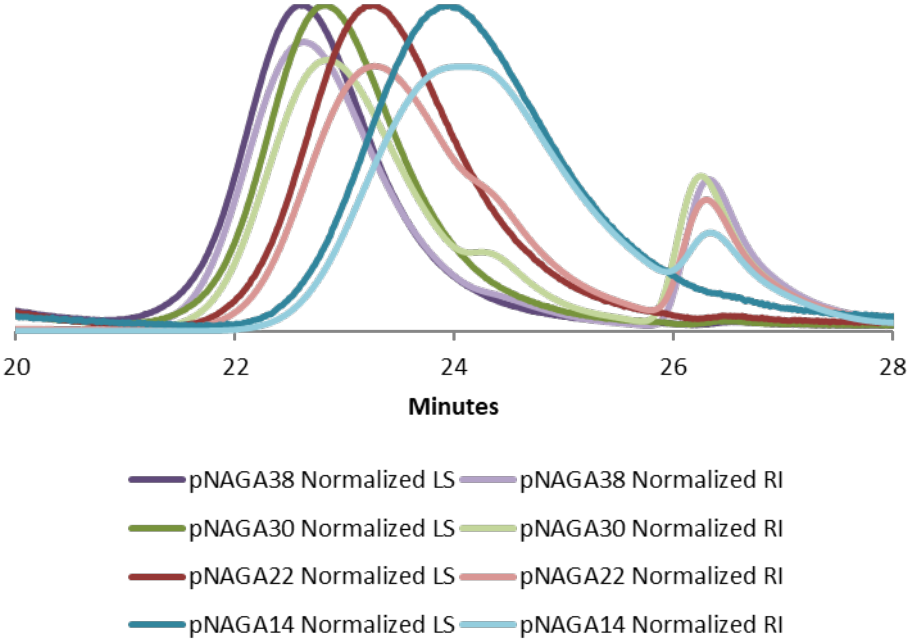

Figure S3. Size exclusion chromatography normalized light scattering and refractive index traces of pNAGA polymers. The shoulders 24.5 min are a result of RAFT termination events.

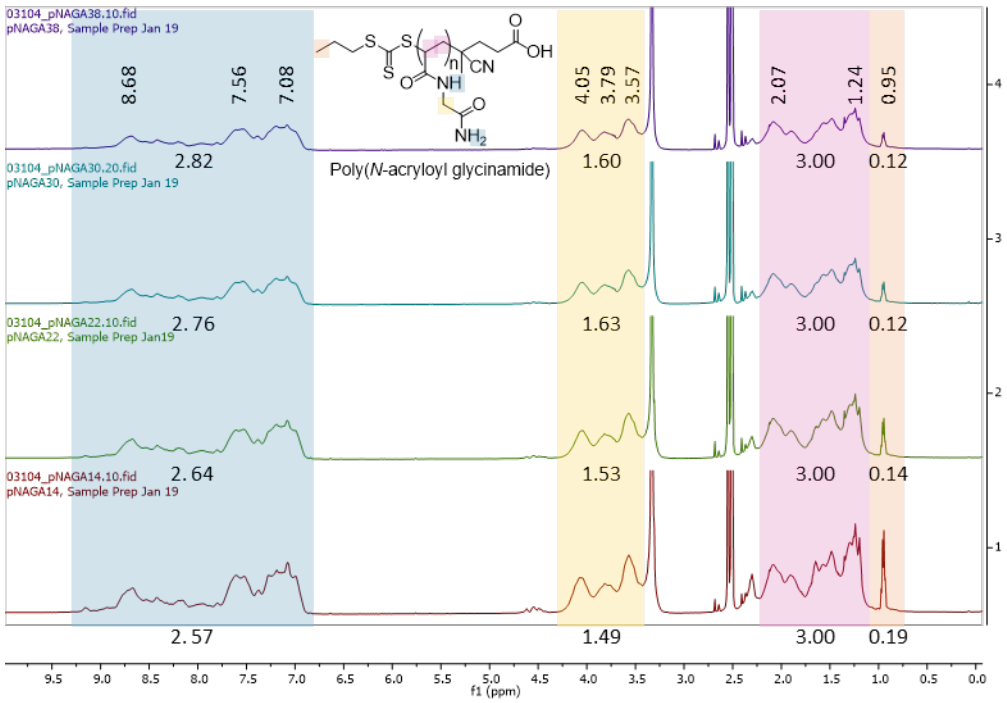

Figure S4. 1H NMR of pNAGA polymers.

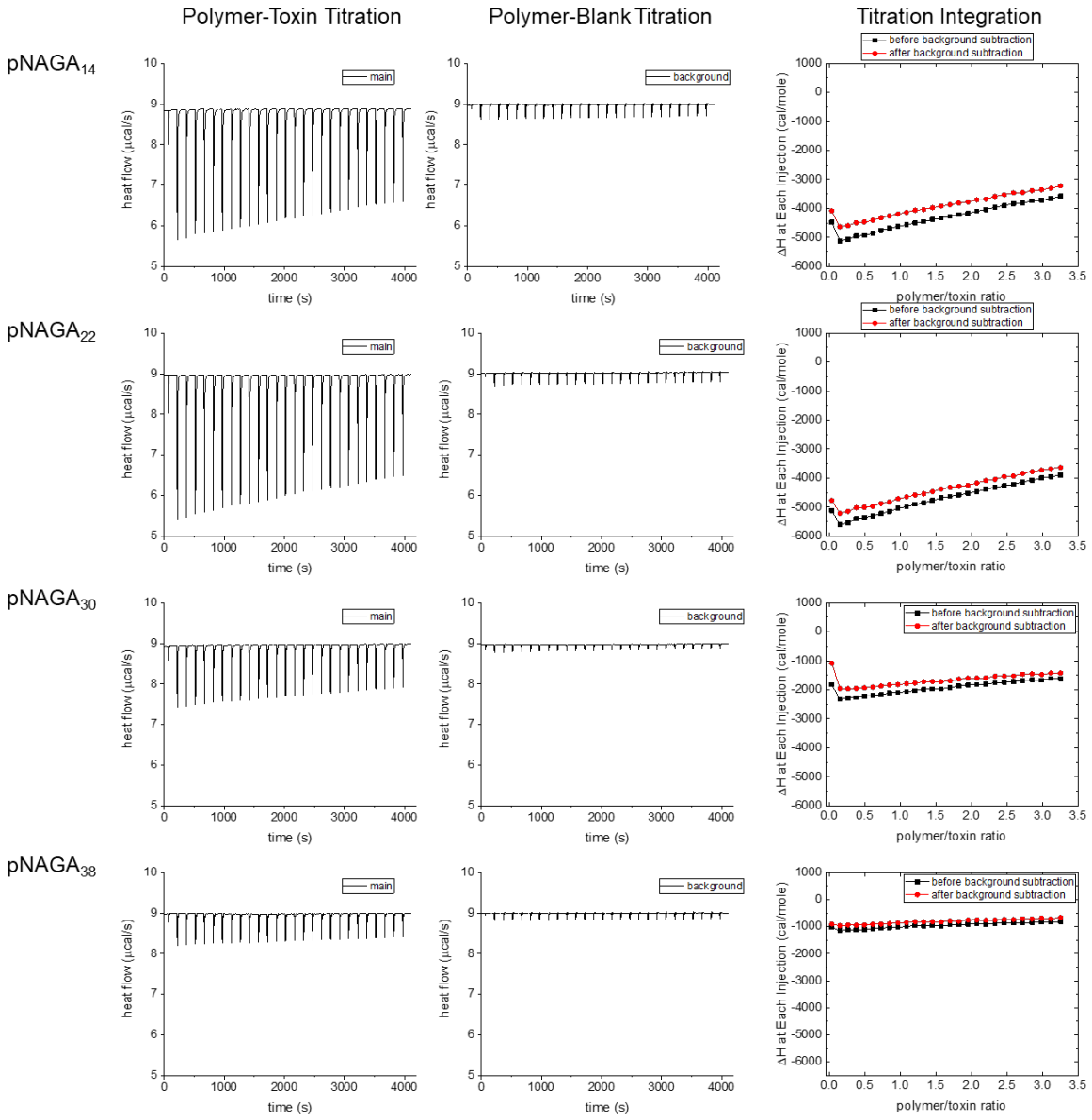

Figure S5. Individual ITC injection and integrated plots for pNAGA series. The integrated plots show the main titration in black and the main after background subtraction in red.

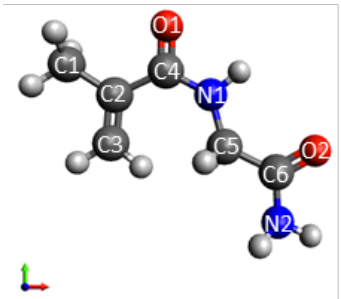

Figure S6. Atomic labels of modeled NMAGA

Table S2. Visually assigned vibrational modes of the monomer NMAGA. Assignments reference atomic labels from Figure S6.

Wavenumber shift (cm^{-1})	Assignment
556	(m) deloc.
598	(m) deloc
611	(m) delocalized twisting C2-C3, N1-C5, C6-N2
630	(w) similar to 611
703	(m) similar to 611, but more localized on C2-C3
736	(m) C1-C2, C2-C4 symmetric stretch and small N1-C5-C6 bending
773	(m) C2-C3 twisting
822	(m) C5-C6 stretching, wagging of H's on N2, C4-N1-C5 bending
896	(w) wagging of H's on C3
925	(w) C1-C2 stretch, rocking of H's on C3
990	(m) rocking of H's on C1, rocking of H's on C3
1035	(w) rocking/wagging of H's on C1, slight twisting of H's on C3
1044	(m) rocking of H's on N2, slight C6-O2 and C6-N2 symmetric stretching
1130	(w) N1-C5 stretch
1187	(m) C4-N1-C5 asymmetric stretch, twisting of C5 H's
1211	(m) C1-C2-C4 asymmetric stretch, rocking of C3 H's, twisting of C5 H's, rocking of N1 H
1248	(m) wagging of C5 H's, C6-N2 stretch
1322	(m) C2-C4 stretch, wagging of N1 H, wagging of H's on C5, C5-C6-N2 asymmetric stretching
1344	(m) C2-C4-N1 asymmetric stretch, C5 H's wagging, C5-C6-N2 asymmetric stretch
1357	(m) wagging of H's on C1
1397	(s) bending of H's on C3 and C1, coupled bending of angle between C1-C2-C4 with C2-C3 stretch
1424	(m) Bending of H's on C1
1446	similar to 1424, but phase of bending is different
1453	bending of C5 H's
1561	(w) O2-C6-N2 symmetric stretch, bending of N2 H's
1631	(m) asymmetric stretching of C2-C3 and C4-O1
1651	(s) predominantly C4-O1 stretch
1702	(w) C6-O2 stretch

The calculated normal Raman spectra of the monomer and anchoring group enabled the identification of pNAGA modes that may be affected by noncovalent binding of AFB1, specifically those of the repeat unit terminal amide. When used in conjunction with the experimental spectra of the four pNAGA molecular weights, the calculated spectra verified pNAGA attachment to the SERS substrate. The known modes of the calculated spectrum revealed spectral changes due to the increasing repeat unit character, relative to anchoring CTA group, with increasing chain length and demonstrated that the full chain resided within the enhancing electromagnetic field SERS substrate. This confirmed all pNAGA chain lengths as valid candidates for AFB1 SERS affinity agents.

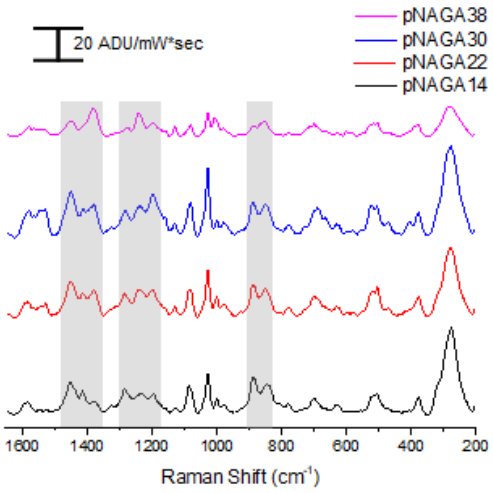

Figure S7. SERS of pNAGA polymers anchored to the FON substrates. Shaded regions identify trithiocarbonate terminated polymer-CTA vibrations that change with increasing polymer length.

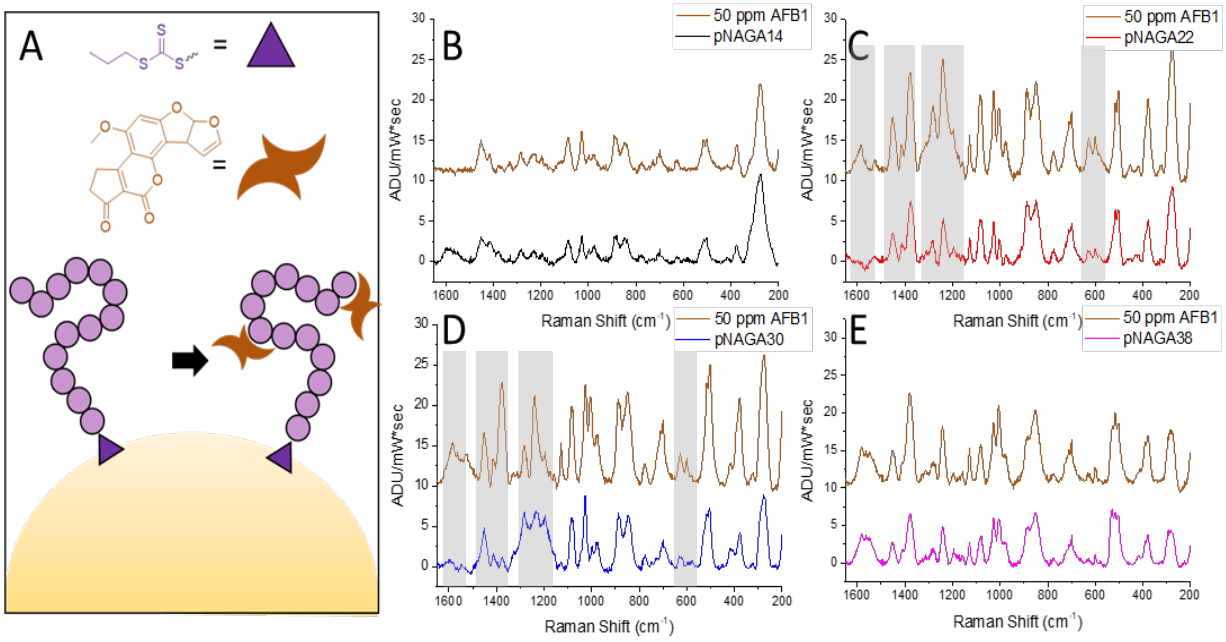

Figure S8. SERS spectra of CTA NAGA polymer at various chain lengths incubated in 50 ppm AFB1. Grey regions denote spectral changes after AFB1 interaction in post-attachment scheme. Spectral changes were not observed at lower concentrations of AFB1.

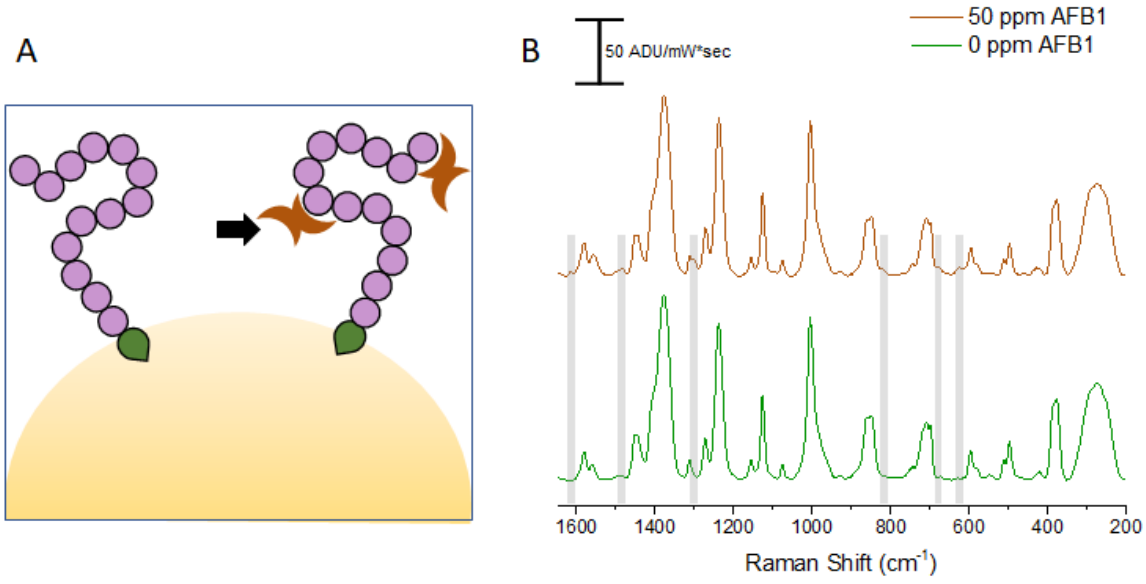

Figure S9. SERS spectra of thiolated $pNAGA_{22}$ polymer at various chain lengths incubated in 50 ppm AFB1. Grey regions denote spectral changes after AFB1 interaction in post-attachment scheme. Spectral changes were not observed at lower concentrations of AFB1.

CTA-only to thiol reduction:

Spectra of the attachment chemistries (CTA and thiol) were collected as a control. A 1 mM solution of CTA-only was made with 4:6 methanol:MQ water solution. The CTA is not water soluble, therefore surface coverage on the FON was not ideal. The FONs were incubated in CTA solution for 18 hours and the same SERS methods, detailed in the manuscript, were used to collect the spectra. The CTA was reduced to a thiol following the same protocol as the reduction performed on the polymer in the manuscript. 0.138g of CPP was used to make a 5 mM solution. This solution was diluted to a 1mM solution for analysis. The FONs were incubated in this solution of reduced CTA for 18 hours and the spectra was collected in the same way as previously mentioned.

As previously discussed in the manuscript, the decrease in magnitude of CTA vibrations should be observed after the reduction of the CTA. Figure S9 exhibits the disappearance or decrease in multiple peaks: a strong and intense peak shift at 518 cm^{-1} matching the 503 cm^{-1} shift (symmetric 'breathing' of CS_2=S bonds), a shoulder peak at 652 cm^{-1} from to the 688 cm^{-1} shift (S-C stretch), a peak at 891 cm^{-1} attributed to the 887 cm^{-1} shift of the C-C stretching of the CPP propyl group, shoulder peak at 1089 cm^{-1}shift matching the 1028 cm^{-1} shift (C=S and C-C symmetric stretch), a peak at 1233 cm^{-1} that matches the 1242 cm^{-1} shift (C=S and CH_2-CH_2 asymmetric stretch), and the 1445 cm^{-1} shift attributed to the trithiocarbonate vibrations at 1451 cm^{-1} shift (CH_3-CH_2 H bending).

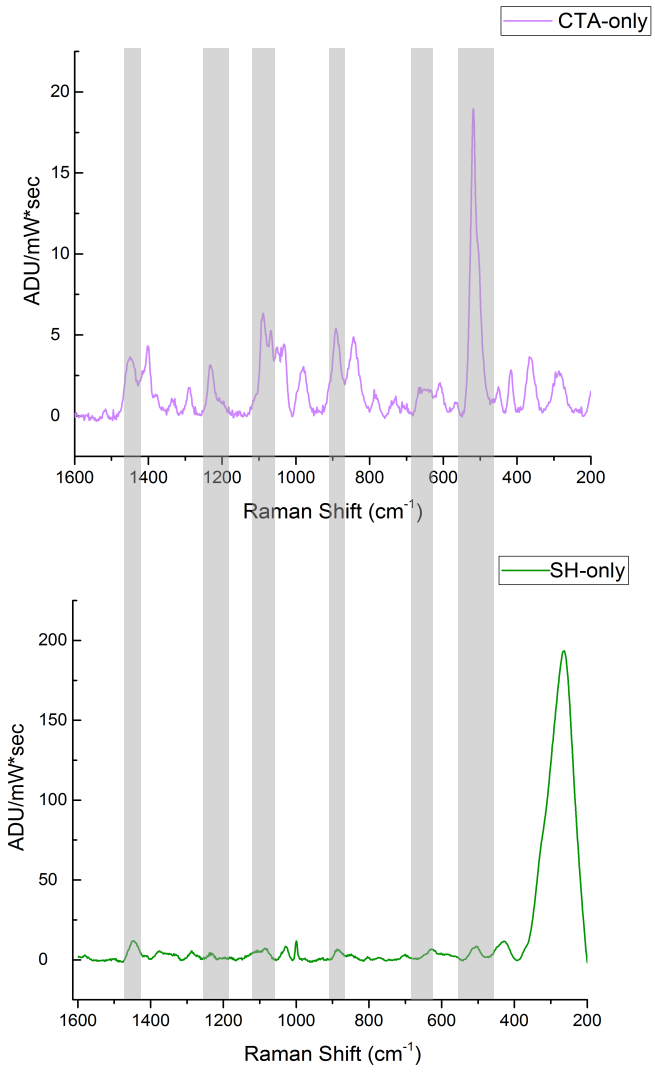

Figure S10. SERS characterization of CTA-only and reduced SH-only FONs.